## Molecular Crystals and Liquid Crystals Science and Technology. Section A. Molecular Crystals and Liquid Crystals

## Molecular and Crystal Structure and Properties of Te-Containing p-Terphenoquinone Analogues

Rui Tamura [a] , Mroyuki Takasuka [b] , Yuya Nagata [b] , Nagao Azuma [b] , Akira Matsumoto [b] , Yoshihiko Sadaoka [c] , Atsushi Gunji [d] , Kazuko Takahashi [d] , Akio Kamimura [e] & Kenzi Hori [e]

[a] Laboratory of Organic Chemistry, Division of Material Science , Graduate School of Environmental Earth Science, Hokkaido University , Sapporo, 060, Japan

[b] Department of Chemistry, Faculty of General Education , Ehime University , Matsuyama, 790, Japan

[c] Department of Applied Chemistry, Faculty of Engineering , Ehime University , Matsuyama, 790, Japan

[d] Department of Chemistry, Faculty of Science , Tohoku University , Sendai, 980, Japan

[e] Department of Chemistry, Faculty of Liberal Arts , Yamaguchi University , Yamaguchi, 753, Japan
Published online: 24 Sep 2006.

PLEASE SCROLL DOWN FOR ARTICLE

and views expressed in this publication are the opinions and views of the authors, and are not the views of or endorsed by Taylor & Francis. The accuracy of the Content should not be relied upon and should be independently verified with primary sources of information. Taylor and Francis shall not be liable for any losses, actions, claims, proceedings, demands, costs, expenses, damages, and other liabilities whatsoever or howsoever caused arising directly or indirectly in connection with, in relation to or arising out of the use of the Content.

This article may be used for research, teaching, and private study purposes. Any substantial or systematic reproduction, redistribution, reselling, loan, sub-licensing, systematic supply, or distribution in any form to anyone is expressly forbidden. Terms & Conditions of access and use can be found at http://www.tandfonline.com/page/terms-and-conditions

# MOLECULAR AND CRYSTAL STRUCTURE AND PROPERTIES OF Te-CONTAINING *p*-TERPHENOQUINONE ANALOGUES

RUI TAMURA,*[1] HIROYUKI TAKASUKA,[2] YUYA NAGATA,[2] NAGAO AZUMA,[2] AKIRA MATSUMOTO,[2] YOSHIHIKO SADAOKA,[3] ATSUSHI GUNJI[4], KAZUKO TAKAHASHI, [4] AKIO KAMIMURA[5] AND KENZI HORI[5]

[1]Laboratory of Organic Chemistry, Division of Material Science, Graduate School of Environmental Earth Science, Hokkaido University, Sapporo 060, Japan, [2]Department of Chemistry, Faculty of General Education and [3]Department of Applied Chemistry, Faculty of Engineering, Ehime University, Matsuyama 790, Japan, [4]Department of Chemistry, Faculty of Science, Tohoku University, Sendai 980, Japan and [5]Department of Chemistry, Faculty of Liberal Arts, Yamaguchi University, Yamaguchi 753, Japan

Abstract  *p*-Terphenoquinone analogues containing a quinonoid type of tellurophene skeleton in the central position have been prepared with a view to developing a new type of organic photoconductive materials having amphoteric redox properties. X-ray structure analysis showed that each molecule exhibited an asymmetric boat conformation owing to the bent structure of the whole ring system and the opposite twisting of two terminal rings. The molecular packing manner in the crystals depends on the substituents on the terminal quinonoid rings. These compounds were electrically amphoteric and afforded radical cation salts and CT complexes by electrochemical or chemical oxidation or by the reaction with an appropriate electron acceptor, respectively. Preliminary experimental results on the photoconductive properties of the neutral compound along with the electrical and magnetic properties of the radical cation salts and CT complexes are described.

# INTRODUCTION

Photoconductive materials are the key component for designing photoelectrochemical devices such as solar cells and electrophotographic printing systems. Particularly, developement of organic photoconductive materials have been closely associated with the progress in electrophotography, in which the original simple single-layer photoreceptors have been replaced by bilayer photoreceptor devices consisting of the charge-generation layer (CGL) and the charge-transporting layer (CTL) to satisfy demanding requirements such as high quantum efficiency of photogeneration, a high charge mobility across the device and a good mechanistic strength.[1]   Since the technology of hole-transporting materials consisting of polymeric films doped with electron donors such as aromatic amines and hydrazones is more advanced than that of electron-transporting ones, to

date most of practical bilayer organic photoreceptors are negatively corona-charged at the surface on the upper hole-transporting layer.   However, the use of the negative corona-charging mode is always accompanied by two indispensable disadvantages; the insufficient discharge stability and the considerable generation of ozone gas harmful to both human and photorecepters.  Therefore, development of positively corona-charged organic photoreceptor devices is desired from the economical and environmental standpoints.  It has been disclosed that unsymmetrical diphenoquinone 1 has sufficient electron affinity, exhibits high chemical stability of the resulting radical anion species and excellent electron-transporting ability, and shows high solubility in organic solvents and high dispersibility in binder polymers mainly due to the less cohesive force between the molecules.[2]    However, it is more desirable if single-layered polymeric films doped with both electron donors and acceptors[3] or more ideally with single component having amphoteric redox properties can possess the sufficient bipolar charge transporting ability in the positively surface-charged fashion, compared with the bilayer systems described above.

Electrically amphoteric five-membered heterocycle-extended quinones, tetrasubstituted *p*-terphenoquinone analogues 2,[4] 3,[5] and 5[6] synthesized recently by us might be promising candidates for single layered photoelectrochemical devices, because (1) they are fairly stable molecules both in the solid state and in solution, (2) they may retain essentially a coplanar conformation for the whole molecule like 3c[5b], (3) they exhibit an intense $\pi-\pi^*$ absorption maximum in the visible wave length region (550 - 600 nm),[5,6] (4) a fine adjustment of the HOMO-LUMO energy split might be possible by judicious choice of the central five-membered heterocycle and the substituents at the $\alpha$-positions of the carbonyl groups in the terminal quinonoid rings,[5c] (5) they are both reducible and oxidizable through multistage electron-transfer reactions,[4,5,6] (6) they may not easily form CT-complexes with electron donors, (7) the corresponding radical anions and the dianions are fairly stable in solution, owing to the existence of the heteroatom in the central ring,[4,5,6] and (8) the corresponding radical cations, which must be more



1
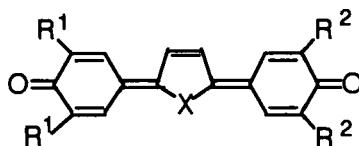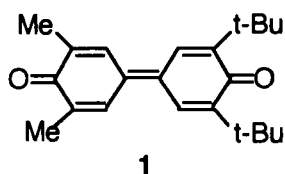
2: X=O     **a:** $R^1 = R^2 = H$
3: X=S     **b:** $R^1 = R^2 = Me$
4: X=Se    **c:** $R^1 = R^2 = t\text{-Bu}$
5: X=Te    **d:** $R^1 = Me; R^2 = t\text{-Bu}$

stable in the solid state than in solution, can be stabilized by changing the central heteroatom (O, S, Se and Te) and the substituents on the terminal quinonoid rings.

Tellurium-containing *p*-terphenoquinone analogues **5b** showed very low oxidation potential (Table II) and fairly high electrical conductivities in its radical cation salts.[6] However, it exhibited intractable poor solubility in organic solvents, probably due to strong intermolecular Te---Te contacts and π–π stacking leading to the aggregation, strictly prevented further application.   Therefore, we focused on dissymmetrically substituted **5d** that would have the reduced cohesive force between molecules resulting in inprovement of solubility in organic solvents.   We here describe the synthesis, structural analysis and electrochemical properties of  **5d**, together with preliminaly experimental results on the photoconductive properties of **5d** and the electrical and magnetic properties of the CT complex and radical cation salt derived from **5d**.


## PREPARATION OF Te-CONTAINING p-TERPHENOQUINONE ANALOGUE (5d)

The synthetic procedure of **5d** is shown in Scheme 1.   To a soution of 1,4-bis(trimethylsilyl)-1,3-butadiyne (0.970 g, 5.00 mmol) in THF (5mL) was added dropwise MeLi (1.05 M ether solution, 5.24 mL, 5.50mmol) at -78°C under argon atmosphere, followed by warming to 25°C over 1 h and additional stirring for  2 h at 25°C.    A solution of anhydrous $ZnCl_2$ (0.780 g, 5.5 mmol) in THF (5 mL) was added to the resulting mono lithium acetylide solution and the mixture was stirred for 2 h at 25°C.    This solution was then transferred to a mixture of 2,6-dimethyl-4-iodo-1-methoxymethyloxybenzene (1.62 g, 5.50 mmol) and Pd(PPh3)4 (0.280 g, 0.25 mmol) in THF (5 mL)  at 25°C and the reaction mixture was stirred overnight at 25°C.   Water (30 mL) was added, and the aqueous mixture was extracted with ether (3 x 30 mL).   The combined organic phase was dried over $MgSO_4$, and concentrated in vacuo.   The residual black oil was passed through short-path silica gel column (hexane)  to  give 0.972 g (68%) of oily crude **6**: ^{1}H NMR (CDCl3) δ 6.98  (s, 2H),  4.95 (s, 2H),  3.55 (s, 3H), 2.22 (s, 6H), 0.22 (s, 9H).

MeLi  (3.57 mL, 3.40 mmol) was added dropwise to a solution of the crude **6** (0.974 g, 3.40 mmol) in THF (5 mL) at -78°C under Ar, and the mixture was warmed to 25°C over 1 h and stirred for 2 h at 25°C. A solution of anhydrous $ZnCl_2$ (0.423 g, 3.40 mmol) in THF (5 mL) was added to the resulting lithium acetylide solution and the mixture was stirred  for 2 h  at 25°C.   This solution was then transferred to a mixture of 2,6-di-*t*-butyl-4-iodo-1-(trimethylsilyloxy)benzene (2.02 g, 5.00 mmol) and  Pd(PPh3)4
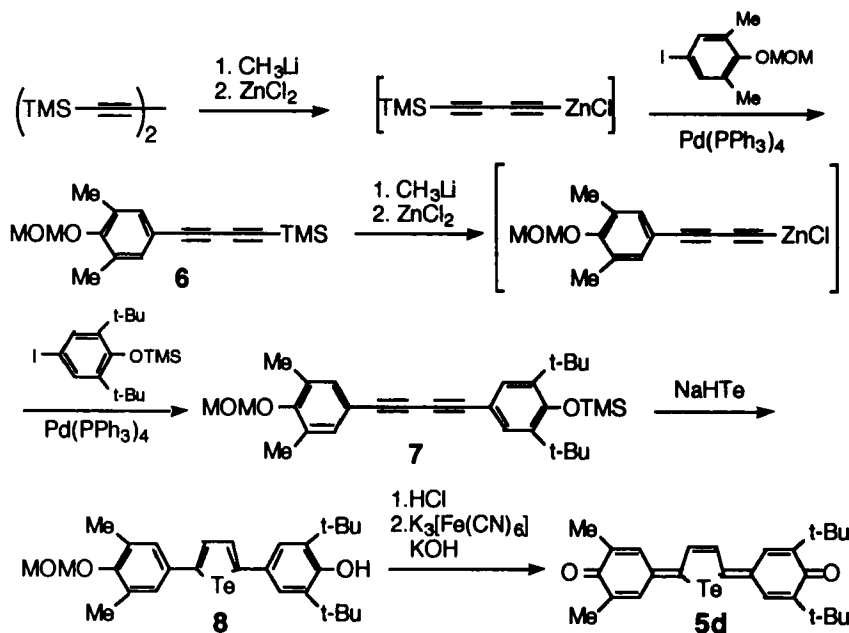
SCHEME 1   Preparation of **5d**.

(0.173 g, 0.15 mmol) in THF (5 mL)  at 25°C and the reaction mixture was stirred overnight at 25°C.   By a similar workup procedure described above,  1.20 g (72%) of crude **7** was obtained as an oil.  **7**: $^1$H NMR (CDCl$_3$) δ 7.43 (s, 2H), 7.33 (s, 2H), 5.01 (s, 2H), 3.63 (s, 3H), 2.23 (s, 6H), 1.34 (s, 18H), 0.33 (s, 9H).

A solution of the crude **7** (0.815 g, 1.66 mmol) in benzene (5 mL) was added all at once to the hot NaHTe solution prepared by refluxing a mixture of powdered tellurium (0.635 g, 4.98 mmol) and NaBH$_4$ (0.440 g, 11.6 mmol) in EtOH (20 mL) for 1 h, and the reaction mixture was refluxed overnight and then cooled to 25°C.   The solvent was removed in vacuo and the residual solid was extracted with CH$_2$Cl$_2$ (3 x 20 mL).   The combined extracts were filtered and concentrated to give  the crude **8** as a yellow powder. To the crude **8** (0.437 g, 0.797 mmol) in THF (8 mL) was  added  conc  HCl  (0.2 mL), and the mixture was stirred for 5 h at 50°C.   After cooling to 25°C, 0.1N aq KOH solution (40 mL) and K$_3$[Fe(CN)$_6$] (1.05 g, 3.19 mmol) was added and the reaction mixture was stirred overnight at 25°C.   Water (30 mL) was added, and the aqueous mixture was extracted with CH$_2$Cl$_2$ (3 x 30 mL).   The combined organic phase was dried over MgSO$_4$, and concentrated in vacuo to give 0.291 g of crude **5d** as a dark blue powder.   Purification by column chromatography on silica gel (20:1 hexane/ethyl acetate) followed by recrystallization from hexane gave  0.175 g  (21 % from **7**) of

analytically pure **5d**: mp 189.5-191.5°C; IR (KBr) 2954, 1589, 1499, 1357, 1199, 1031 cm$^{-1}$; UV-vis (CH$_2$Cl$_2$) λmax nm (log ε) 355 sh (3.48), 434 (4.04), 448 (4.04), 482 sh (3.77), 591 (4.52). $^1$H NMR (CDCl$_3$) δ 7.83 (d, J= 6.4Hz, 1H), 7.78 (d, J=6.4Hz, 1H), 7.54 (dd, J=2.6, 1.3Hz, 1H), 7.52 (d, J=2.6Hz, 1H), 6.77 (dd, J=2.6, 1.4Hz, 1H), 6.66 (d, J=2.6Hz, 1H), 2.10 (d, J=1.2Hz, 3H), 2.13 (d, J=1.2Hz, 3H), 1.36 (s, 9H), 1.33 (s, 9H) ; $^{13}$C NMR (CDCl$_3$) δ 186.9, 185.9, 151.0, 150.9, 150.4, 147.0, 141.5, 141.1, 138.6, 137.8, 135.9, 135.5, 134.9, 134.6, 127.6, 124.0, 35.6, 35.5, 29.6, 29.5, 16.8, 16.7. Anal. Calcd for C$_{26}$H$_{30}$O$_2$Te: C, 62.19; H, 6.02. Found: C, 62.51; H, 6.09.

**5d** showed high solubility in most organic solvents.

## MOLECULAR AND CRYSTAL STRUCTURES OF p-TERPHENOQUINONE ANALOGUE (5c and 5d)

The single crystals of **5c** and **5d** of good quality for X-ray crystallographic analysis were obtained by recrystallization from acetone and hexane, respectively, whereas attempted recrystallization of **5b** from various solvents failed to produce the single crystal, giving only powder. The crystals of **5c** were red-brown blocks, while **5d** black needles. The crystal data for **5c** and **5d** summarized in Table I show that each molecule in the crystals of both **5c** and **5d** has chirality. Although **5c** and **5d** essentially retain a coplanar conformation for the whole molecule, they exhibit the slight boat conformation with dihedral angles of 8.8° and -3.6° (Figure 1a), and 1.9° and -5.7°(Figure 2a), respectively, between the mean plane of the central five-membered ring and each mean plane of the two terminal six-membered rings. Therefore, the dihedral angles between the mean planes of the two terminal six-membered rings for **5c** and **5d** are 10.3° and 7.2°, respectively. This boat conformation and the opposite twisting of the two terminal six-membered rings to the central five-membered ring with twisting angles of 5° and 8°, and 2° and 9° for **5c** and **5d**, respectively, (and dissymmetrical substitution in the case of **5d**) would be responsible for the molecular chirality observed in the crystal state. The boat conformation of **5c** is in contrast to the chair conformation observed for the corresponding sulfur-analogue **3c**,[5b] where the mean planes of the terminal six-membered rings incline 9.1° and 11.1°, respectively, from that of the central five-membered ring and hence the twisting angle between the mean planes of the two terminal rings is 1.8°. Furthermore, it has been found that **5c** is composed of enantiomerically pure crystals, while the crystals of **5d** and **3c** were racemic in the crystallographic sense.

As to the crystal structure, **5d** has the distinct molecular stacking along the *a* axis with alternate intermolecular face-to-face distances of 3.6 and 3.8Å (Figure 2b),  although short intermolecular Te---Te contacts are not observed because of the alternate  stacking of two enantiomers oppositely directed to each other so as to avoid the  steric hindrance between di-*t*-butyl-substituted six-membered rings.   Therefore, the observed intermolecular interaction in the crystal of **5d** is one-dimensional in this direction.   On the other hand,  no noticeable intermolecular interaction was observed in **5c** and  the shortest intermolecular face-to-face distance of **5c** was as long as 10Å, the length of the *b*  axis (Figure 1b).

TABLE I     Selected crystallographic parameters for **5c** and **5d**.

|  | **5c** | **5d** |
|---|---|---|
| space group | $P2_1$ | $P2_1/c$ |
| *a*, Å | 9.446 (2) | 8.095 (2) |
| *b*, Å | 10.259 (2) | 18.103 (2) |
| *c*, Å | 17.750 (3) | 16.493 (2) |
| $\beta$ | 91.26 (1) | 103.46 (1) |
| Z | 2 | 4 |
| R/Rw | 0.040/0.037 | 0.040/0.037 |

(a)                                        (b)
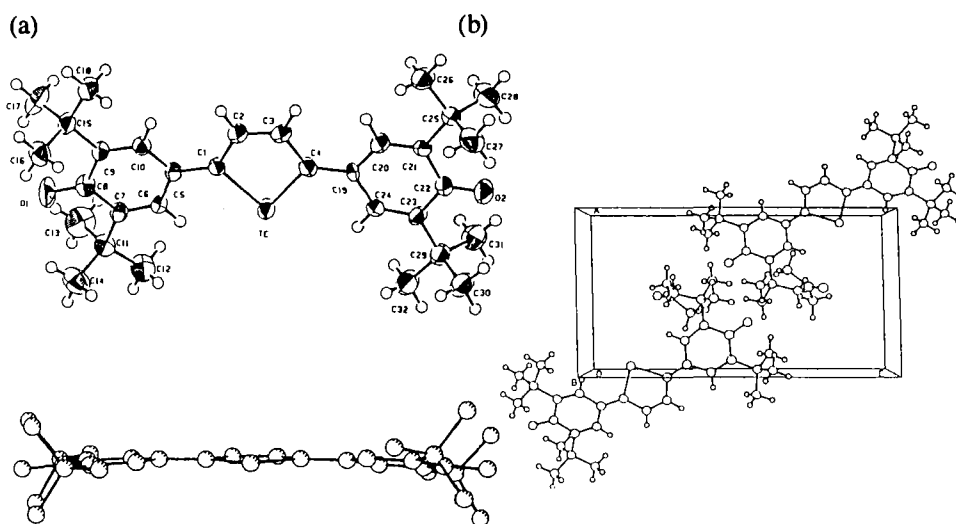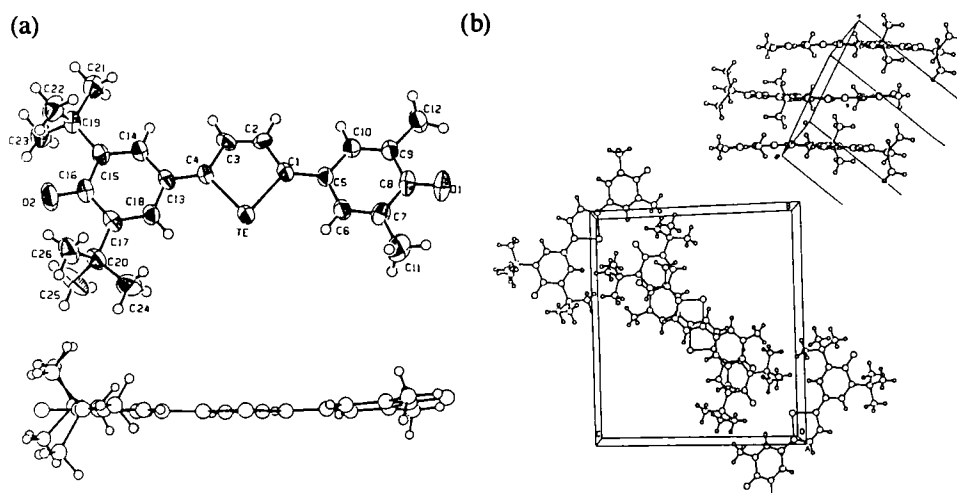


FIGURE 1   (a) Molecular and (b) crystal structure of **5c**.

(a)                                              (b)



FIGURE 2    (a) Molecular and (b) crystal structure of **5d**.

Thus, it is concluded that from the crystal data **5d** seems to be superior to **5c** as a conducting material.

## ELECTROCHEMICAL PROPERTIES AND UV-VIS ABSORPTION SPECTRA

The cyclic voltammogram of **5d** in benzonitrile exhibited two reversible reduction waves with half-wave reduction potentials of -0.57 and -0.74V and an irreversible oxidation
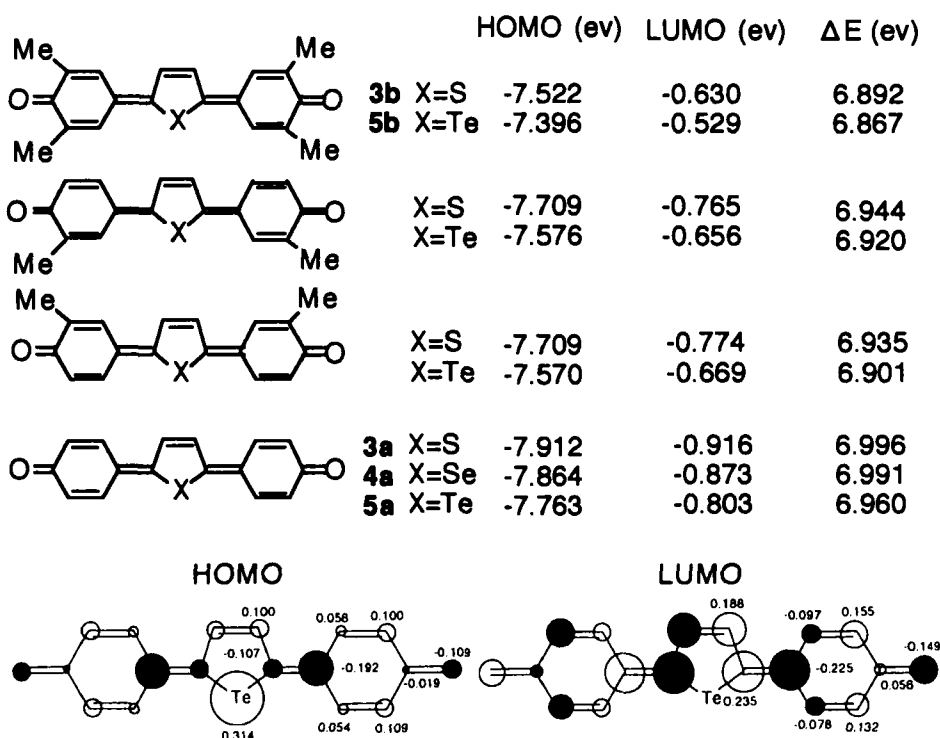
TABLE II    Redox potentials and UV-vis spectra of **1, 3, 4** and **5**.[a]

| Compd. | Solvent | $E_1^{red}$ | $E_2^{red}$ | $E_{pa}^{ox}$ | $E_1^{sum}$ | λmax [nm] (logε) |
|--------|---------|-------------|-------------|---------------|-------------|------------------|
| **1** | $CH_2Cl_2$ | -0.48 | - | - | - | 422 (5.20)[j] |
| **3b**[b,c] | PhCN | -0.37 | -0.44 | 1.24[f] | 1.61 | 546 (4.87)[c,i] |
| **3c**[b,c] | PhCN | -0.47 | -0.67 | 1.28[g] | 1.75 | 558 (4.90)[c,i] |
| **5b**[d] | PhCN | -0.68[e] | | 0.63[h] | 1.31 | 592 (4.47)[d,j] |
| **5c**[d] | PhCN | -0.59 | -0.73 | 1.04[h] | 1.63 | 593 (4.79)[d,j] |
| **5d** | PhCN | -0.57 | -0.74 | 1.15[f] | 1.72 | 591 (4.52)[j] |

[a] Potentials (V vs. SCE) were measured by CV with 0.1 M (n-Bu)4NClO4 at 25°C (scan rate, 50 mV/s). $E_{pa}^{ox}$ is measured based on the anodic peak current. $E_1^{sum} = E_{pa}^{ox} - E_1^{red}$. [b] 0.1M (n-Bu)4NBF4 was employed for CV measurement. [c] Cited from ref 5b. [d] Cited from ref 6. [e] Two electron reduction. [f] Irreversible. [g] Reversible. [h] Quasi-reversible. [i] Measured in $CH_3CN$. [j] Measured in $CH_2Cl_2$.

wave with an oxidation peak at 1.15V vs SCE electrode (Table II).   The oxidation potential of **5d** is similar to that of **5c**, but quite different from that of **5b**.  The reduction behaviour of **5d** is also similar to that of **5c** showing two-step one-electron rerduction potentials.   The reduction potentials of **5d** is more negative by ca 0.1V than those of **1** and **3c**.

Ab initio frontier molecular orbital calculations of unsubstituted charcogen-containing *p*-terphenoquinone analogues **3a**, **4a** and **5a** indicate that the energy level of the LUMO of the tellurium-analogue is higher than those of the corresponding sulfur and selenium analogues.  However, the energy difference between the HOMO and LUMO levels in tellurium-analogue **5a** (ΔE=6.960 eV)  is slightly smaller than those of sulfur-analogue **3a** (6.996 eV) and selenium-analogue **4a** (6.991 eV) by the virtue of the relatively high HOMO level ascribing to the low valence state ionization potential of tellurium as shown in Scheme 2.[7]  Furthermore, it is also noteworthy that placing methyl groups on the four α-positions of the carbonyl groups in the terminal quinonoid rings induces the more increase of the HOMO level due to the electron-releasing effect of

| | | HOMO (ev) | LUMO (ev) | ΔE (ev) |
|---|---|---|---|---|
| **3b** | X=S | -7.522 | -0.630 | 6.892 |
| **5b** | X=Te | -7.396 | -0.529 | 6.867 |
| | X=S | -7.709 | -0.765 | 6.944 |
| | X=Te | -7.576 | -0.656 | 6.920 |
| | X=S | -7.709 | -0.774 | 6.935 |
| | X=Te | -7.570 | -0.669 | 6.901 |
| **3a** | X=S | -7.912 | -0.916 | 6.996 |
| **4a** | X=Se | -7.864 | -0.873 | 6.991 |
| **5a** | X=Te | -7.763 | -0.803 | 6.960 |



SCHEME 2   HOMO and LUMO levels of **3**, **4** and **5** and MO coefficients of **5a**.

methyl groups than that of the LUMO level, eventually resulting in the decrease of the energy difference between the two levels, i.e., **3b** ($\Delta E$=6.892 eV) and **5b** (6.867 eV) (Scheme 2).

In accord with the MO calculations, **5d** showed a lower oxidation potential by 0.09 and 0.13 V and the longer wavelength of the first excitation absorption maximum by 45 and 33 nm than **3b** and **3c**, respectively. This high electron-donating ability of **5d** is mainly ascribed to the low valence state ionization potential of tellurium, since the extent of $\pi$ delocalization of the 5p$\pi$ electrons on the tellurium atom through carbon framework stabilizing the corresponding radical cation is considered to be low because of the disparate size of the tellurium and carbon.[9] Since the largest MO coefficient resides on the central tellurium atom in the HOMO of **5a** as shown in Scheme 2, the unpaired electron should be localized considerably on the tellurium atom in the radical cation of **5**.

## PHOTOCONDUCTIVE PROPERTIES OF 5d

Since **5d** showed high dispersibility in binder polymers such as poly(4,4'-cyclohexylidenediphenyl carbonate (PC-Z) and poly(N-vinylcarbazole) (PVK) as well as high solubility in various organic solvents, preliminary measurements of the photocunductive properties of **5d** were performed. The HOMO and LUMO energy diagram of **5b**, **5c** and **5d** in the solid state was obtained by measuring the ionization potentials of the powdered materials by means of a photoionization method and by calculating the energy gap between the HOMO and LUMO levels from the absorption tails in the electronic spectra of thin films of the materials dispersed in PCZ, as shown in Figure 3. Apparently both the HOMO and LUMO levels of **5d** shows the intermediate values between **5b** and **5c**. From this diagram it is expected that the ionization potential of **5d** is low enough to release an electron by photoirradiation, and this feature might incude both the charge separation and transfer between the same molecules. Therefore, in order to evaluate the single-component bipolar charge transporting ability of **5d** upon photoirradiation, the time-of-flight measurement of **5d** dispersed (50 wt %) in PC-Z was attempted by using a nitrogen laser pulse.[2b] As a result, the single-component of **5d** did not show either of the electron-transport nature or the hole-transport nature in this experiment. Further studies with the aim of designing molecules having amphoteric redox properties so as to induce both the charge separation and transport between the same molecules upon photoirradiation are under investigation.
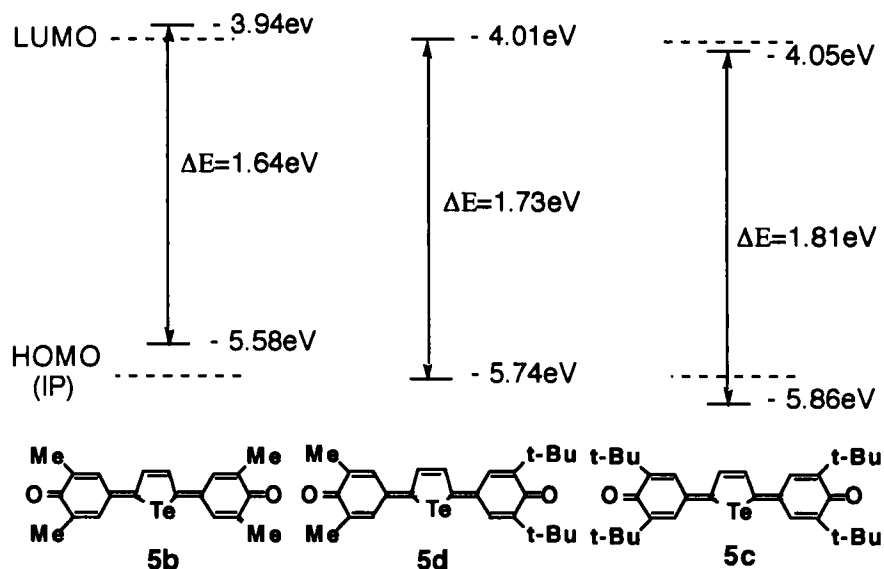
FIGURE 3  Energy diagram of **5b**, **5c** and **5d** in the solid state.

## MAGNETIC AND ELECTRICAL PROPERTIES OF RADICAL CATION SALTS AND CT-COMPLEXES

In order to evaluate the electron-donating ability of **5d** and the stability of its radical cation species, the radical cation salt and CT complex of **5d** were prepared by chemical oxidation or by the reaction with an appropriate electron acceptor, respectively.    Although electrochemical oxidation of **5d** failed to give any radical cation salt, chemical oxidation of **5d** with $(p\text{-}BrC_6H_4)_3NSbCl_6$[10] provided a radical cation salt, $\mathbf{5d}\text{·}[SbCl_6]_{1.2}$, in $CH_2Cl_2$ as a dark black powder.   The black powdered CT complex $\mathbf{5d}\text{·}TCNQF_4$ was also prepared by the reaction of **5d** with $TCNQF_4$ in hot $CH_2Cl_2$.   Their ESR spectra in the solid state were shown in Figure 4.   Although these radical species were fairly stable in the solid state under argon atmosphere, these solution in organic solvents did not exhibit ESR spectra. The radical cation salts $\mathbf{5d}\text{·}[SbCl_6]_{1.2}$ and $\mathbf{5d}\text{·}TCNQF_4$ were insulators, exhibiting conductivities less than $10^{-8}$ S cm$^{-1}$ measured by the two-probe method on compressed pellets.

In contrast, radical cation salts of **5b** prepared by the electrochemical oxidation and powdered CT complex $\mathbf{5b}\text{·}TCNQF_4$ showed higher conductivities of $\sigma\sim10^{-4}$ and $10^{-5}$ Scm$^{-1}$, respectively.[6]        The radical cation $\mathbf{5b}\text{·}[SbCl_6]_{0.5}$ prepared by chemical

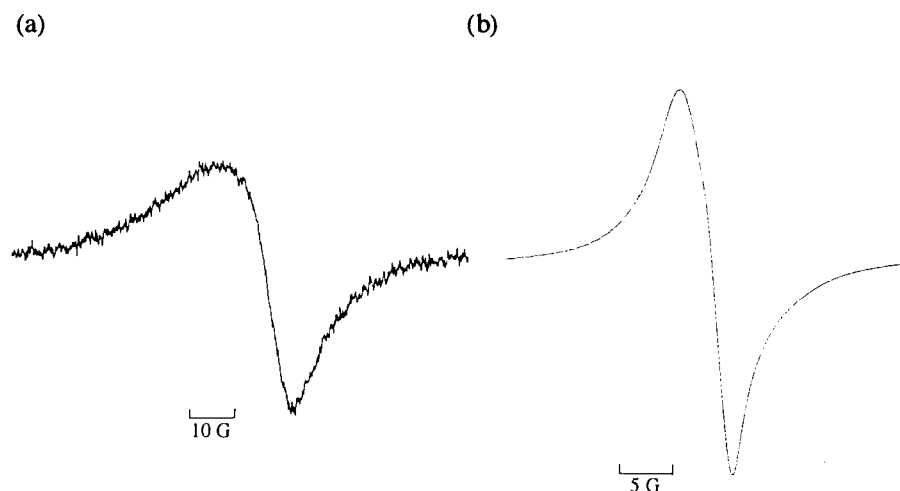(a)                                              (b)



FIGURE 4   ESR spectrum of (a) **5d**·[SbCl$_6$]$_{1.2}$ and (b) **5d**·TCNQF$_4$ in the solid state.

oxidation was again an electrical insulator, although the ESR spectra of this radical cation salt was observed (g=2.0037, $\Delta$H=8.7G). These results are summarized in Table III. Thus, it is noted that although the radical cation salts are uniformly stable in the solid state, the electrical conductivity of these salts are highly dependent on the manner of preparation and the structure of the **5**.

TABLE III   Electrical conductivity and ESR spectral data of radical cation salts and CT complexes derived from **5b** and **5d** in the solid state.[a]

| Compd. | Conductivity $\sigma$ (S cm$^{-1}$) | g-Value | $\Delta$H (gauss) |
|---|---|---|---|
| **5d**·[SbCl$_6$]$_{1.2}$[b] | < 1.0 x 10$^{-8}$ [d] | 2.0038 | 16.2 |
| **5d**·TCNQF$_4$[b] | < 1.0 x 10$^{-8}$ [d] | 2.0033 | 4.7 |
| **5b**·[SbCl$_6$]$_{0.5}$[b] | < 1.0 x 10$^{-8}$ [d] | 2.0037 | 8.7 |
| **5b**·TCNQF$_4$[b] | 1.15 x 10$^{-5}$ [e] | 2.0035 | 5.4 |
| **5b**·[BF$_4$]$_2$[c] | 1.13 x 10$^{-4}$ [e] | 2.0021 | 11.1 |
| **5b**·[ClO$_4$]$_{1.1}$[c] | 1.53 x 10$^{-4}$ [e] | 2.0020 | 10.1 |
| **5b**·PF$_6$[c] | 1.53 x 10$^{-4}$ [e] | 2.0020 | 13.4 |

[a] Measured at 25°C.   [b] Obtained by the reaction with (p-BrC$_6$H$_4$)$_3$NSbCl$_6$ in CH$_2$Cl$_2$ at 25°C.   [c] Obtained by electrochemical oxidation, see ref 6.   [d] Measured by two probe method.   [e] Measured by four probe method, see ref 6.

## ACKNOWLEDGMENT

## REFERENCES

1.  (a) K-y. Law, Chem. Rev., 93, 449 (1993). (b) P. M. Borsenberger and D. S. Weiss, Organic Photoreceptors for Imaging Systems (Marcel Dekker, New York, 1993) .
2.  (a) Y. Yamaguchi, H. Tanaka and M. Yokoyama, J. Chem. Soc., Chem. Commun., 222 (1990). (b) Y. Yamaguchi and M. Yokoyama, Chem. Mater., 3, 709 (1991).
3.  Y. Yamaguchi, T. Fujiyama, H. Tanaka and M. Yokoyama, Chem. Mater., 2, 341 (1990).
4.  K. Takahashi, A. Gunji and K. Akiyama, Chem. Lett, 863 (1994).
5.  (a) K. Takahashi and T. Suzuki, J. Am. Chem. Soc., 111, 5483 (1989). (b) K. Takahashi, T. Suzuki, K. Akiyama, Y. Ikegami and Y. Fukazawa, J. Am. Chem. Soc., 113, 4576 (1991). (c) K. Takahashi and T. Sakai, Chem. Lett. 157 (1993).
6.  (a) R. Tamura, Y. Nagata, H. Shimizu, A. Matsumoto, N. Ono, A. Kamimura and K. Hori. Adv. Mater., 5, 719 (1993).
7.  The MO calculations were performed using the LANL1DZ basis set[8] in the Gaussian 90 program. The geometries were optimized with $C_{2v}$ symmetry (all geometrical parameters were fully optimized).
8.  (a) P. J. Hay, W. R. Wadt, J. Chem. Phys., 82, 270 (1985). (b) W. R. Wadt, P. J. Hay, ibid, 82, 284 (1985). (c) P. J. Hay, W. R. Wadt, ibid, 82, 299 (1985).
9.  (a) K. A. Lerstrup and L. Henriksen, J. Chem. Soc., Chem. Commun., 1102 (1979). (b) M. Renson, in The Chemistry of Organic Selenium and Tellurium Compounds, Vol. 1, edited by S. Patai and Z. Rappoport (Wiley, 1986), Chap. 13, pp. 399-516.
10. F. A. Bell, A. Ledwith and D. C. Sherrington, J. Chem. Soc. (c), 2719 (1969).